Winter, J., Fotios, S., & Völker, S.

Gaze direction when driving after dark on main and residential roads: Where is the dominant location?

Winter, J., Fotios, S., & Völker, S. (2016). Gaze direction when driving after dark on main and residential roads: Where is the dominant location? Lighting Research & Technology, 49(5), 574–585. https://doi.org/10.1177/1477153516632867

Gaze direction when driving after dark on main and residential roads: Where is the dominant location?

J Winter Dipl-Ing[a], **S Fotios** PhD[b], **S Völker** Prof Dr-Ing[a]
[a]Fachgebiet Lichttechnik, Technische Universität Berlin, Berlin, GERMANY
[b]School of Architecture, University of Sheffield, Sheffield, UK
j.winter@tu-berlin.de

Keywords: mesopic luminance, eye movement, adaptation, driving after dark

Abstract

CIE JTC-1 has requested data regarding the size and shape of the distribution of drivers' eye movement in order to characterise their visual adaptation. This article reports the eye movement of drivers along two routes in Berlin after dark, a main road and a residential street, captured using eye tracking. It was found that viewing behaviour differed between the two types of road. On the main road eye movement was clustered within a circle of approximately 10° diameter, centred at the horizon of the lane. On the residential street eye movement is clustered slightly (3.8°) towards the near side; eye movements were best captured with either an ellipse of approximate axes 10° vertical and 20° horizontal, centred on the lane ahead, or a 10° circle centred 3.8° towards the near side. These distributions reflect a driver's tendency to look towards locations of anticipated hazards.

1 Introduction

The aim of CIE Joint Technical Committee JTC-1 is to investigate implementation of the CIE recommended system for mesopic photometry defined by CIE 191[1]. This article responds to the JTC-1 request for data regarding the shape and size of the part of the visual field into which a driver's visual gaze tends to fall, these data being used to characterise the visual adaptation of drivers.

Gaze behaviour analysis has been used to investigate where car drivers look[2-3], for example to determine gaze behaviour when steering[4]. The JTC-1 proposal is to use the visual field capturing the majority of eye movements as the field for estimating adaptation luminance. This discussion includes questions of whether the suitable field of view relevant to the adaptation state of a driver is circular or elliptical in shape, whether the size is close to that of the fovea (2°) or whether additional areas of peripheral vision should be taken into account, perhaps field sizes of 10° or 20°, or whether areas such as the road surface or the vehicle windscreen area lead toward a better estimate of adaptation.

In one study[5] this was done by first video recording the driver's field of view when driving along an urban road after dark and then recording eye tracking whilst test participants watched a video on a monitor in a laboratory. A limitation of this approach is that, for pedestrians at least, eye movement when walking in a natural setting does not match those found when watching a video of the same setting[6]. Cengiz et al[7] did record eye tracking whilst driving in order to investigate the effect of size of a circular field (subtending 1°, 5°, 10°, 15° and 20° at the eye) on adaptation luminance but did not consider visual fields of shape other than circular.

Uchida[8] used a numerical simulation method for estimating the state of peripheral adaptation as required for calculating mesopic luminances[1]. His simulation takes input from luminance distribution, eye movement, surrounding luminance (veiling luminance) and an assumed measurement field. For scenes with few potential glare sources, it was found that the road surface luminance provided a good approximation of a driver's adaptation, with an average error of only 2.6% between road surface luminance and simulated adaptation luminance. However, for scenes with a larger number of bright sources, potential glare sources (the 'urban' scenes), there was a large degree of error, increasing rapidly with an increase in the distribution (standard deviation) of eye movements.

In this article, drivers gaze behaviour in inner-city environments after dark was investigated using eye tracking. This was done through secondary analysis of the data captured by others[9] in which test participants were asked to drive a motor car along a pre-defined route without any specific task other than safely driving towards a goal whilst their eye movement was captured using eye tracking. The analysis used all available gaze direction data, both fixations and saccades, collectively referred to below as eye movement data.

2 Method

Described here is the apparatus and procedure used by Böhm[9]. Drivers' eye movements were recorded using a head-mounted eye tracking system (Ergoneers Dikablis). This apparatus has two cameras, one facing the driver's field of view and one facing the driver's eye as shown in Figure 1. Before each trial the eye tracking system was calibrated by instructing fixation onto distinctive objects within the visual field whilst the vehicle was stationary in a parking lot. The manufacturer states an angular resolution accuracy of < 0.5° when the eye tracking device is calibrated at the start of each trial by fixation on three fixed positions, the standard procedure for eye tracking. This procedure was followed by Böhm, with an additional secondary check of this calibration with each test participant. The apparatus recorded with a frequency of 25 Hz resulting in 1.8 recorded eye movement data points per meter when driving at 50 km/h or 3 recorded data points per meter when driving 30 km/h.

The head-mounted eye tracking apparatus used here leads to a head-centred coordinate system because the origin of the coordinate system moves in conjunction with head movement[10]. For JTC-1 an environment-centred system of coordinates is needed, e.g. vehicle-centred or road-centred. Road-centred means that gaze locations are represented in world frame coordinates. When the car is on a straight road (as is the case for the current study), the car-centred system and the road-centred system are similar. Therefore a third camera (TechnoTeam LMK 98-4) was mounted behind the driver's seat (Figure 2) to enable conversion from the head-centred system to the car/road-centred system. This translation was undertaken using the Augmented Reality Marker (ARMarker) fitted to the vehicle dashboard on the left-hand side of the steering wheel following the method of Kato and Billinghurst[11]. This third camera was static and aimed to capture the scene observable through the front windscreen. Following previous work, we considered only eye movement toward the road ahead. Eye movements toward the dashboard may also affect the

state of adaptation and the significance of this will be examined in further work.

Eye movements were monitored whilst driving along two sections of road in Berlin as described in Table 1. All test participants followed the same route and the test was carried out in Summer, starting after sunset (i.e. at 2230 CEST). One section of road was a main traffic route (Otto Suhr Allee - OS) having four lanes, separated carriageways, some parked vehicles on the right-hand side of the road and in-between the two carriageways, and intersections with traffic lights. The total length for which eye movement was recorded was 1460 m, this being 650 m and 810 m in the forward and reverse directions respectively. The second section of road was a residential street (Eschenallee - EA) having two lanes without markings, with cars parked on both sides and intersections where the right-of-way is to the right. The total length for which eye movements were recorded was 1140 m, this being 570 m in both the forward and reverse directions. Eye movements were collated for travel in both directions.

The data were collected from 23 test participants, comprising 14 females and 9 males aged between 22 and 73 years (mean = 37 years, SD = 16). Six were relatively inexperienced drivers, having reported less than 10,000 km total driving experience. The test participants were informed that they were participating in a scientific experiment but were naïve as to the research objectives and were remunerated.

3 Visualisation of eye movement distribution

The aim of this work is to identify whether the distribution of drivers eye movement can be categorised by a simple geometric shape. The first approach to analysis employed heat maps to reveal the spread of distributions and suggest possible geometries for subsequent evaluation with quantitative methods.

The data recorded were the locations of drivers' eye movements. Following past work[5,7] these data are presented as heat maps[12] essentially being a 2D-histogram using colour to denote relative magnitude rather than the height of a bar. To draw these it was necessary to extract the raw data (eye movement coordinates) from the eye tracking software and place these within the field of view using the ARMarker i.e. the eye movement data point locations in image coordinates within the head mounted eye tracking videos were transformed into image coordinates of the fixed-forward perspective of the single image from camera 3 located behind the driver's seat (Figure 3).

The eye movement heatmaps for both roads are shown in Figure 4. These illustrate that for the main road (OS) the contour capturing 95% of eye movement is roughly elliptical, but the area of greatest eye movement density (50% and 25% contours) tends toward circular, aiming straight ahead from the driver. For the residential road (EA) the distribution of eye movement is approximately elliptical. Drivers gaze behaviour appears to follow different patterns on these two types of road. The eye movement heatmaps reported by Cengiz et al[7] also suggest ellipses rather than circles but they did not focus on that issue.

4 Distribution of eye movement

Figure 5 illustrates the distribution of these eye movements for two roads along the horizontal and vertical dimensions. In the vertical dimension the difference is small. However, for the horizontal dimension, eye movement in the residential road is more widely distributed than on the main road. In particular, for the main road the focus of attention is the centre of the road ahead, while in the residential road there is a tendency to look also at the near side, the location of potential pedestrians and of junctions where priority is given to those entering the road.

Pairwise t-tests comparing the two types of road for the 23 drivers suggest a significant difference in the standard deviation of horizontal eye movement distribution ($p<0.001$) and a significant difference in offset from the centre line of the road ahead ($p<0.001$). In the vertical dimension the t-test does not suggest a significant difference in distributions ($p=0.44$) or in offset from centre ($p=0.25$) between the two roads. This confirms the differences observed in Figure 4. EA is more elliptical and OS is more circular (or even rectangular) and also EA is shifted to the right (as indicated by the circle in Figure 5 which represents the centre of the lane ahead).

Given that there is an apparent difference in eye movement behaviour between roads EA and OS, a post-hoc analysis was carried out to investigate whether there were significant differences between different sections of the same type of road. Four discrete sections of each road type were established (OS1-OS4 and EA1-EA4), these defined as the distance between two successive lamp posts, and were distances of 28 m and 40 m for OS and EA respectively. This analysis was carried out using the eye tracking data for only 13 of the 23 drivers on account of the requirement for a high amount of manual labelling: comparing using ANOVA the eye movement for this subset of 13 drivers with those of all 23 drivers did not suggest significant differences ($p\geq0.59$) in any case of horizontal or vertical distribution or offset from centre and thus it was assumed to be a

reasonably representative sample.

Analysis of these discrete sections using ANOVA, for the two road types separately, did not suggest differences in the distribution of eye movement nor the offset from centre to be significant ($p \geq 0.13$) except for one case: on road OS there was a significant difference in offset from the centre line of the road ahead in the horizontal dimension ($p=0.003$). Pairwise comparisons using the Tukey HSD test suggest that the differences in offset for OS are that OS1 lead to a different offset than OS3 ($p=0.04$) and OS4 ($p=0.002$) (Table 2). The difference between OS1 and OS2 is close to significant ($p=0.10$) but differences between OS2, OS3 and OS4 are far from significant ($p \geq 0.42$). Thus in section OS1 drivers were tending to look to the nearside but in OS2, OS3 and OS4 they were looking slightly to the left of centre. Reasons for looking to the right-hand side in OS1 are that there were locations for potential hazards, e.g. approaching a traffic light controlled intersection, a road junction, and cars parked on the side of the road. In OS3 and OS4 there were potential hazards (parked cars) on the left hand side, between the two carriageways.

These analyses suggest that different types of road (i.e. a main road and a residential road) led to different patterns of eye movement. Figure 4 suggests that these may be circular on the main road (OS) and elliptical on the residential road (EA). Past studies[4] suggest that drivers tend to look towards locations necessary in order to prevent accidents. This behaviour can be seen in the current data, as they follow expectation of likely hazards for which the driver is searching. On the main road (OS) they are tending to look straight ahead, approximately to the centre of the lane (or the rear of the vehicle in front), but may look towards a specific location for expected hazards, hence towards the right-hand side in OS1 (the location of pedestrians and to prevent accidents with vehicles coming from the right hand side, which have the right of way) and towards the left-hand side in OS2-OS4 (cars parked between the two traffic lanes). In the residential street (EA) they are tending to look toward the nearside of the road. The next section analyses the effectiveness of circular and elliptical visual fields at capturing eye movement on the two types of road.

5 Approximation by basic geometric shapes

In order to assess how well eye movement behaviour can be described by a simple shape, some common shapes were considered for estimating the adaptation state (Table 3). These consist of shapes often used in lighting technology (2° and 10° circles), hypotheses proposed in meetings of

CIE JTC-1[13] (2°/10° and 10°/20° ellipses, whole windscreen area, and road surface). These tentative ellipse sizes may be somewhat arbitrary; to better match the recorded eye movement distributions, alternative ellipses were examined with axes dimensions of size one and two standard deviations of eye movement (1 SD and 2 SD respectively). For analyses of circles and ellipses, these are assumed centred on the lane ahead and at the horizon, this being done to simplify later application in measurement software, although the actual centres of the eye movement data had a horizontal and vertical offset from that point, as shown in Figure 5.

Signal detection theory (SDT) was used to assess the effectiveness of these shapes on a per pixel basis of the forward looking image by classifying each eye movement data point and pixel. All data points were counted as real positives (RP) and all pixels containing no eye movement data as real negatives (RN). The discrete binary classification marked each eye movement data point as true positive (TP) if the pixel containing the data point fell within the shape, as false negative (FN) if the pixel containing the data point fell outside the shape, false positive (FP) if a pixel within the shape did not contain a data point and true negative (TN) for pixels outside the shape without data points (Figure 6).

Two quantities were determined from these data, the false positive rate (fpr) and the true positive rate (tpr) (equations 1 and 2)[14]. Tpr considers the number of eye movement data points which fell within the shape and is the ratio of the number of data points within the shape to the total number of data points (i.e. within and outside of the shape): a tpr approaching unity means the shape encapsulates the majority of eye movement data points. Fpr considers those pixels which were not the subject of a visual gaze, and is the ratio of non-fixated pixels within the shape to the total number of non-fixated pixels: a fpr approaching zero means that the shape had few non-fixated pixels as these tended to fall outside of the shape. Note that for TN and FP the empty (non-viewed) pixels were each scored as one, whereas for TP and FN these viewed pixels were scored as the number of eye movement data points on that particular pixel. The receiver operating characteristic (ROC) space was used to assess whether the shapes of Table 3 provide a satisfactory fit to the distribution of eye movements according to fpr and tpr. ROC is a common tool to assess the outcome of binary classifiers[15], showing fpr on the x axis and tpr on the y axis.

$$fpr = FP / (FP + TN) \quad (1)$$

$$tpr = TP / (TP + FN) \quad (2)$$

The shape best encapsulating drivers' gaze behaviour has tpr approaching unity and fpr approaching zero and would thus lie in the upper left region. However, that approach does not penalise false negatives and false positives within one value (if not taken into account the result would show the bigger the assumed visual field, the better the tpr, only slightly worsening the fpr, because of the relatively large number of RN, ending up with still small Euclidian distances to the upper left). Real negative eye movement data points do not exist, therefore the number of pixels within the luminance image (1031 · 1371) minus the number of pixels with data points were used to calculate TN and fpr. That means TN depends on the actual size of the image and is mainly influenced by the focal length of the utilized lens (Figure 7). A common measure to quantify the results of classification where TN is undefined is the f1-score[16].

The f1-score (equation 3) was therefore used as a second assessment parameter, this having the advantage that it does not require TN as an input value. Equation 3 is based on Van Rijsbergen's effectiveness measure[17]. F1-scores range from 0 to 1; a score of 1 indicates the shape is a perfect classifier, with all eye movement data points captured by the shape, no data points outside the shape boundary, and all available data points within the shape being used; a score of zero indicates the shape give a poor definition of the eye movement data point distribution. If only tpr were used as the assessment parameter the outcome would favour the largest shape - it would incorporate the most data points with no penalty for false positives. Using only fpr would favour the smallest shape because it would incorporate the fewest false positives.

$$f1\text{-}score = 2 \cdot TP / ((2 \cdot TP) + FN + FP) \qquad (3)$$

Figure 8 shows the ROC space for the two road types and the location within these for the eye movement shapes listed in Table 3. For both the main road and the residential street the 10° / 20° ellipse, the 2 SD ellipse and the window area were those located closest to the ideal upper-left location of the graph: for the main road, the 10° circle was also in this location. Considering the f1-score, this was lower for the window than for the other three shapes, these shapes having a similar f1-score.

For the residential street (EA) the ellipse of size either 10° / 20° or 2 SD performed approximately equally well at capturing eye movement data points. For simplicity of application, the 10° / 20°

ellipse may be preferable to that defined by 2 SD. For the main road (OS) drivers eye movement data points were captured by an ellipse of size 10° / 20°, an ellipse of size 2 SD or by a 10° circle. The 10° circle is proposed here, with the assumption that the f1 score takes priority over the ROC location, meaning that the circle is a better measure than the ellipse. However, having a common field shape for both road types may simplify application and therefore further evaluation should consider whether assumption of an elliptical field introduces significant error.

For Figure 8, the tentative shapes were centred at the horizon of the lane ahead. Analysis of the gaze location distributions show that fixations were slightly offset from this position, a shift of 0.5° vertical, 0.3° horizontal on the main road, and 0.1° vertical, 3.8° horizontal on the residential street. If the tentative shapes are instead centred on these offset locations, the results for the main road (OS) remain in the same order, this offset being relatively small. On the residential street (EA) the order based on the f1-score would change, favouring the 10° circle over the 10° / 20° ellipse (See Table 4). What this does is show a driver's desire on a residential road to look towards the near-side, e.g. toward the kerb, pedestrians on the footpath, or an approaching side road junction.

These conclusions suggest that different types of road have different eye movement patterns and thus JTC-1 needs to consider different adaptation field shapes. A field size analysis such as that of Cengiz et al[7] should consider an elliptical field in addition to a circular distribution. One caveat is that the primitive shapes do not represent the actual Gaussian distribution of the data, because they are flat, equally weighting the area within.

6 Age and Experience

Age and experience are likely to affect eye movement because of the deterioration of vision with age[18] and the assumption that experience feeds the anticipatory probabilistic model of the world of a driver[18]. In the current article we used the data from Böhm[9] which included 23 drivers of a wide age range (22 to 73 years) and both experienced and inexperienced drivers. Of these, only four might be considered elderly (aged, 59, 66, 70 and 73 years) with the remainder being aged less than 50 and having a mean age of 31 years. The mix of age and experience in this sample were intended to represent approximately the gaze behaviour of the population of drivers.

Table 5 shows past studies of eye tracking and driving. Where age and experience are reported these samples have tended to represent younger drivers, and there is a mix of experienced and

novice drivers. Experience brings familiarity with a given environment and an expectation of where significant hazards are found, and thus we would expect the distribution of gaze behaviour to be more compact for experienced drivers than for novice drivers. This can be seen in the results of two studies[2,19]. For example, Mourant and Rockwell[19] found that the central gaze direction of their novice drivers was lower and farther to the right (i.e. towards the kerb) than for experienced drivers, suggesting this was due to sampling of the curb in order to verify or estimate vehicle lane alignment. In contrast, Falkmer and Gregersen[20] found that at intersections experienced drivers tended to spread their fixations over a much wider horizontal distribution than did inexperienced drivers. Maltz and Shinar[18] identified that older drivers tend to need longer visual search times than younger drivers in order to extract the same amount of information of a traffic scene. They also found that the attention of the younger was distributed more evenly across the scene, whereas the older drivers focused on a smaller subset of areas within the presented image – a suggestion of experience (with age) leading a more compact field of view. If both older and younger, and novice and experienced, drivers are expected to use a road, and since these distinctions may affect gaze behaviour, then all groups should be included in the sample included in an experiment.

7 Summary

The aim of this work is to analyse driver's eye movement on main roads and residential streets after dark. Heat maps were used to reveal the spread of distributions and statistical analysis to compare viewing behaviour between the two types of road. With a novel shape classification approach we identified the most suitable field shape approximating the eye movement data.

The heat maps suggest that gaze behaviour differs between the main road and the residential street: the 25 % and 50 % contours on the main road were approximately circular, whereas on the residential street the 25 % and 50 % contours were approximately elliptical. Descriptive statistics indicate, that standard deviation and offset to the centre of the lane at the horizon differ on the horizontal dimension, but not on the vertical dimension, which was confirmed by inferential statistics. A post-hoc analysis revealed, that viewing behaviour differed at one subsection of the main road, but was consistent on the other subsections of the main road, as well as on the residential street.

Signal detection theory was used to investigate the optimum field of view shape. For the residential road there is a tendency to look slightly to one side of straight ahead, i.e. towards the near side. SDT suggested the optimum shape to be a 10° / 20° ellipse if the centre of fixation is assumed to be the centre of the lane ahead, or a 10° circle if the centre of fixation is placed slightly to the right in accordance with the recorded data. For design purposes, the former may be the more simple assumption. On the main road the 10° circle was slightly better than the 10° / 20° ellipse. Favouring a common shape for both types of road would ease a potential practical application, however it would have to be assessed whether that lead to additional error.

The tentative field shapes represent the eye movement of the fovea, whereas for the application of the mesopic luminances the peripheral vision is of interest. The method proposed by Uchida[8] is one approach that might address the issues of peripheral adaptation.

Acknowledgement

The authors thank Michael Böhm for providing the raw eye tracking data for this study.

References

1 CIE:191. *Recommended system for mesopic photometry based on visual performance*. Technical report, Commission Internationale de l'Eclairage, 2010.

2 Mourant RR, Rockwell TH. Mapping Eye-Movement Patterns to the Visual Scene in Driving: An Exploratory Study. *Human Factors: The Journal of the Human Factors and Ergonomics Society*. 1970;(12):81–87.

3 Stahl F. [Congruence of eye movement between virtual and real drives - Validation of a night drive simulator] (In German). Master's thesis, L-LAB / TU Ilumenau, 2004.

4 Land MF, Lee DN. Where we look when we steer. *Nature*. 1994;(369):742–744.

5 Heynderickx I, Ciociou J, Zhu XY. Estimating eye adaptation for typical luminance values in the field of view while driving in urban streets. In: *Towards a new century of Light*. CIE; 2013. p. 41–47.

6 Foulsham T, Walker E, Kingstone A. The where, what and when of gaze allocation in the lab and the natural environment. *Vision Research*. 2011;51(17):1920–1931.

7 Cengiz C, Kotkanen H, Puolakka M, et al. Combined eye-tracking and luminance measurements when driving on a rural road: towards determining of mesopic adaptation luminance. *Lighting Research and Technology*. 2014;46(6):676–694.

8 Uchida T. Adaptation luminance simulation for CIE mesopic photometry system implementation. In: *CIE Session 2015 Manchester*. CIE; 2015. p. 307 – 316.

9 Böhm M. [Final report of project no. ff-fp0328: Visibility of reflective garments] (In German). Technical report, FG Lichttechnik, Technische Universität Berlin, 2013.

10 Pinker S. Visual cognition: An introduction. *Cognition*. 1984;18(1-3):1–63.

11 Kato H, Billinghurst M. Marker Tracking and HMD Calibration for a Video-based Augmented Reality Conferencing System. Human Interface Technology Laboratory, University of Washington; 1999.

12 Holmqvist K, Nyström M, Andersson R, et al. *Eye Eye Tracking: A Comprehensive Guide to Methods and Measures*. Oxford University Press; 2011.

13 Minutes of the 4th Meeting of CIE JTC-1: Implementation of CIE 191 Mesopic Photometry in Outdoor Lighting. Tuesday, December 17, 2013. 2.00-4.00 p.m. CET. Webex-meeting

14 McNicol D. *A Primer of Signal Detection Theory*. London: Allen & Unwin (Publishers), 1972.

15 Fawcett T. An introduction to ROC analysis. *Pattern Recognition Letters*. 2006;27(8):861–874.

16 Hripcsak G, Rothschild AS. Agreement, the F-Measure, and Reliability in Information Retrieval. *Journal of the American Medical Informatics Association*. 2005;12(3):296–298.

17 van Rijsbergen C J. *Information Retrieval* (2nd ed.). London: Butterworth & Co (Publishers) Ltd. 1979.

18 Maltz M, Shinar D. Eye movements of younger and older drivers. *Human Factors: The Journal of the Human Factors and Ergonomics Society*. 1999;41(1):15–25.

19 Mourant RR, Rockwell TH. Strategies of Visual Search by Novice and Experienced Drivers. *Human Factors: The Journal of the Human Factors and Ergonomics Society*. 1972;14(4):325–335.

20 Falkmer T, Gregersen NP. A Comparison of Eye Movement Behavior of Inexperienced and Experienced Drivers in Real Traffic Environments. *Optometry and vision science*. 2005;82(8):732–739.

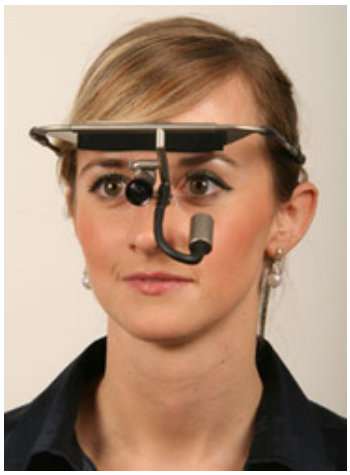

Figure 1. The Ergoneers Dikablis head-mounted eye tracking apparatus.

Figure 2. Photograph of the interior of the test vehicle to illustrate the location of the fixed camera (mounted behind the driver's seat) and the augmented reality markers (ARMarkers), here located on the left-hand and right-hand sides of the steering wheel.

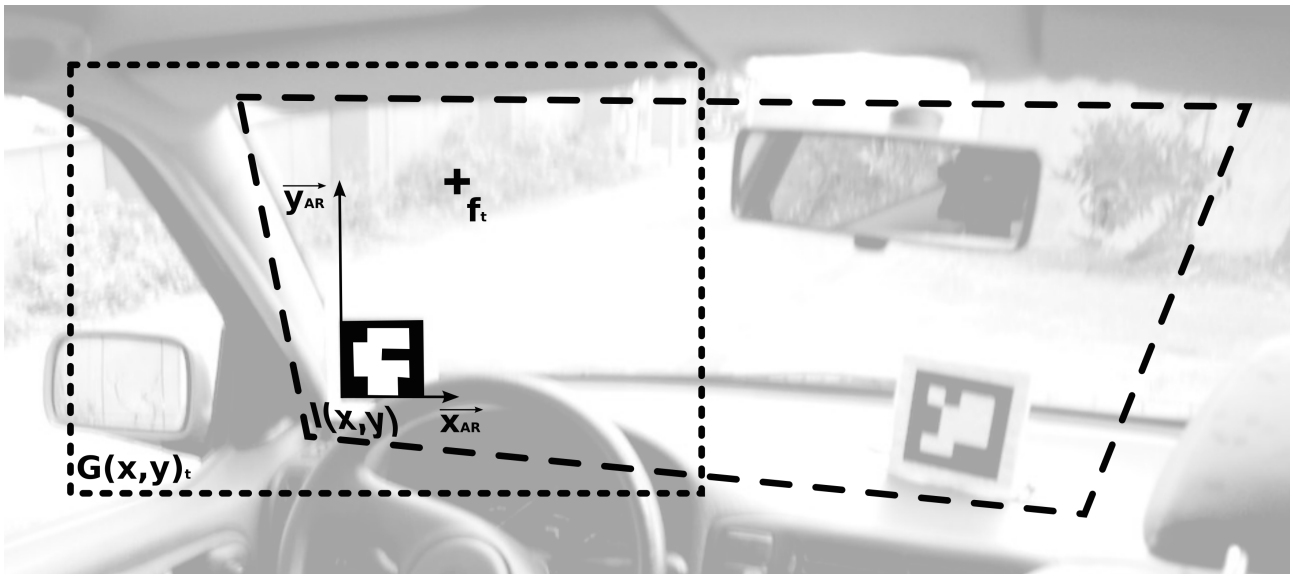

Figure 3. Sketch of the coordinate transformation of an eye movement data point from the eye tracking image **G(x,y)t** to the image taken of the fixed-forward perspective **I(x,y)**. Image **G(x,y)t** contains an eye movement data point **ft** at time **t** – note that this field of view is dynamic and varies with head movement. The image coordinate of the data point **ft** is being transformed into the ARMarker's vector space with the origin O in one corner and the standard basis defined by the edges of the ARMarker: $\overrightarrow{Of_t} = \overrightarrow{x_{AR}} + \overrightarrow{y_{AR}}$. Finally each data point is cumulated by being inverse transformed from the ARMarker's vector space into image coordinates of the static fixed-forward perspective image **I(x,y)**.

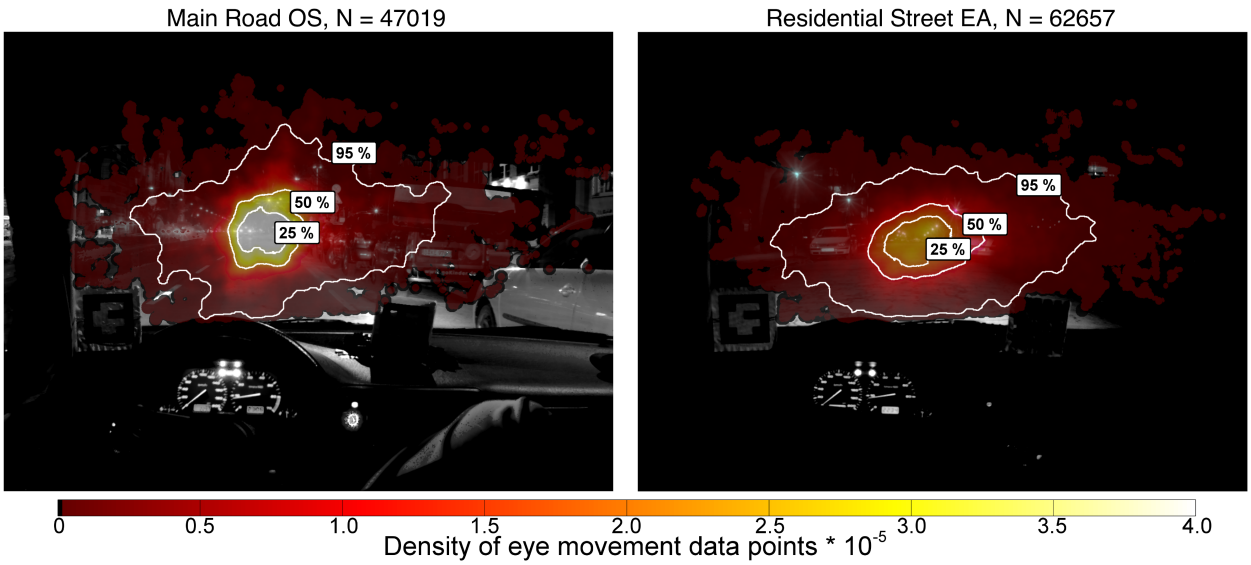

Figure 4. Density Distribution of eye movement data points for main road OS (left) and residential street EA (right) for the 23 subjects. Contours show the 25 %, 50 % and 95 % percentiles. Note: The background image shows for context one particular part of the specific section, although the data shown in the overlain heat map was accumulated along the complete track.

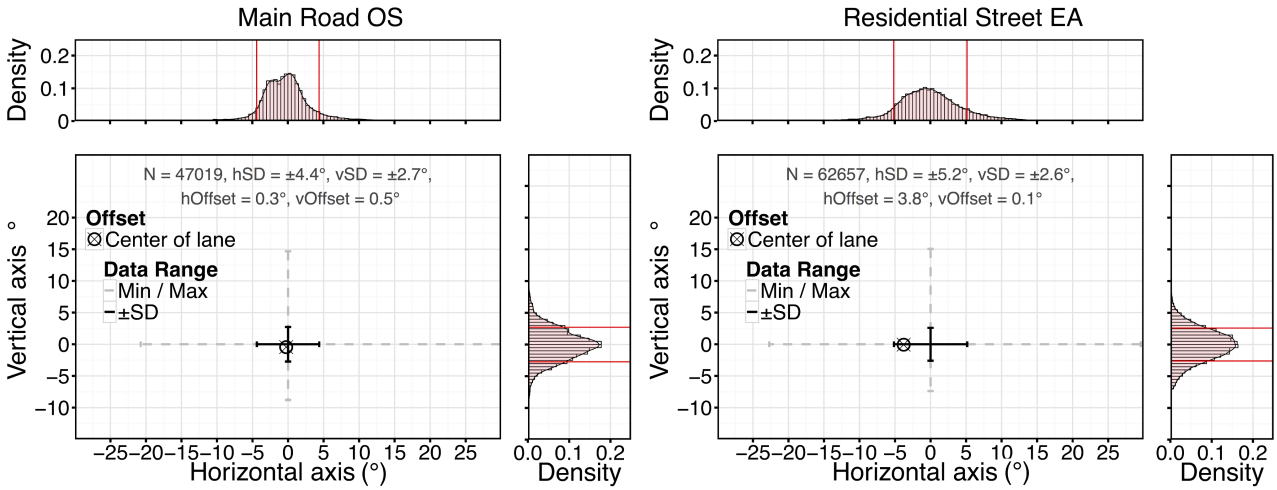

Figure 5. Descriptive statistics for main road OS and residential street EA for the 23 subjects, centred at the horizontal / vertical mean value. Offset represents the vertical / horizontal shift from the centre of the lane at the horizon. Note: the circle shows the centre of the lane ahead.

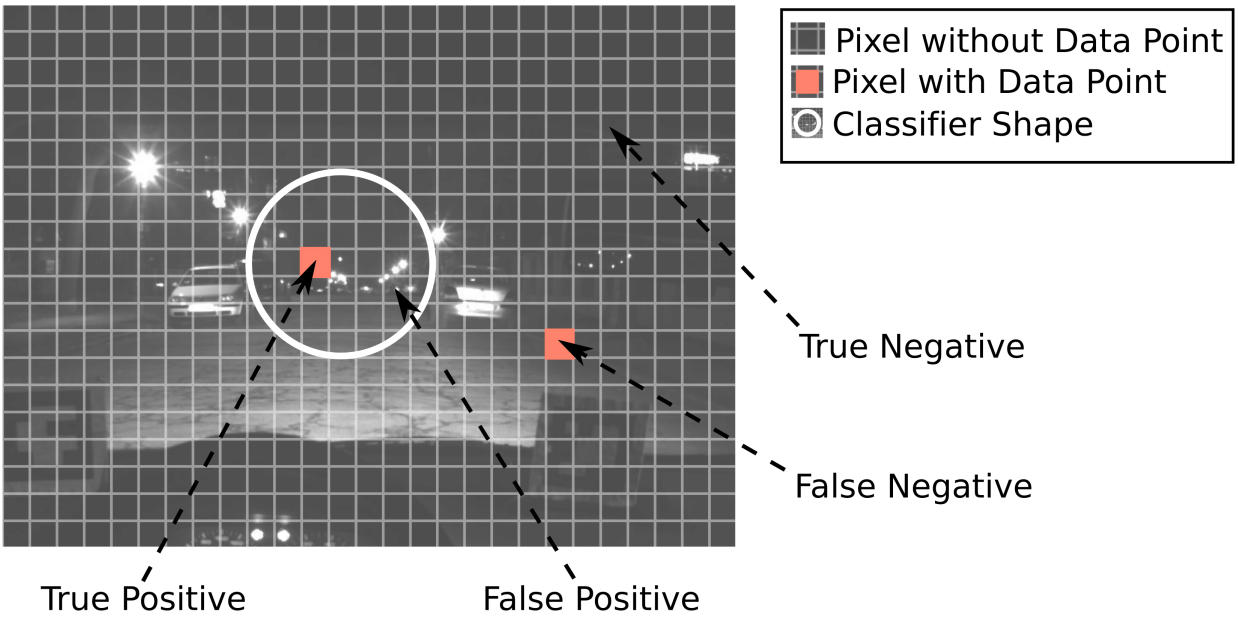

Figure 6. Illustration of per pixel classification. Each eye movement data point on a pixel within the shape was counted as a true positive (TP); data points on a pixel outside of the shape were counted as false negatives (FN); pixels within the shape upon which there were no data points were counted as false positive (FP) and pixels without data points outside the shape were true negatives (TN).

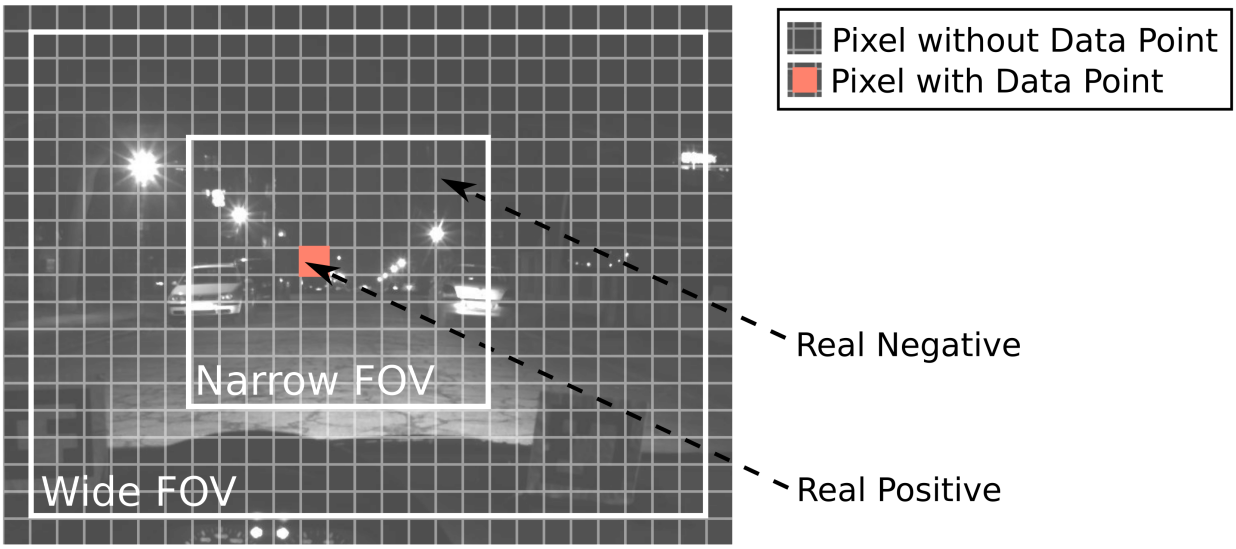

Figure 7. The number of real negatives (RN) depends on the number of pixels of the whole image minus the number of pixels with eye movement data points. The wider the field of view (FOV) of the lens, the higher the number of RNs.

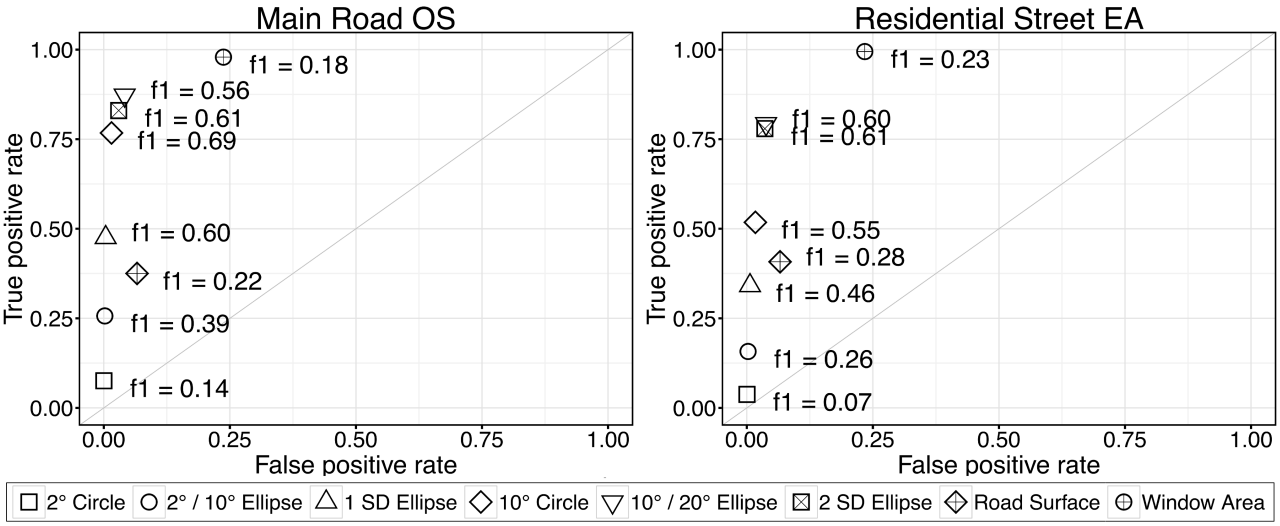

Figure 8. Receiver operating characteristic (ROC) plot for the tentative visual field shapes. These data are for the main road OS (left) and the residential street EA (right) for all 23 test participants. Each tentative eye movement field is centred at the horizon of the lane ahead.

Table 1. Description of the two roads in which eye tracking was recorded.

Name of road	Type of road	Carriageway	Length of road section	Light source*	Speed limit
Otto Suhr Allee (OS)	Main traffic route	Dual	1.46 km	HM	50 km / h
Eschenallee (EA)	Residential area	Single	1.14 km	Gas	30 km / h

*Note: HM = High pressure Mercury; Gas = gas lighting.

Table 2. Horizontal offset of the eye movements for subsections of the main road OS for 13 subjects.

Subsection	Mean (standard deviation)
OS1	1.73 (1.9)
OS2	-0.19 (2.4)
OS3	-0.50 (1.8)
OS4	-1.45 (2.1)

Table 3. Definition of eye movement areas considered in this analysis. The circles / ellipses were positioned at the centre of the lane on the horizon. Note: (i) SD = standard deviation. (ii) Several proposals for adaptation field size were raised at the 2012 meeting of JTC-1 but were not officially recorded.

Name	Description	Source
2° Circle	Circle of diameter 2°	2° standard observer
10° Circle	Circle of diameter 10°	10° standard observer
2° / 10° Ellipse	Ellipse of axes 2° vertical and 10° horizontal	JTC-1, CIE 2012 conference, Hangzhou
10° / 20° Ellipse	Ellipse of axes 10° vertical and 20° horizontal	JTC-1, CIE 2012 conference, Hangzhou
1 SD Ellipse	Ellipse of axes 1 SD in vertical and horizontal directions. • OS: 5.4° vertical / 8.8° horizontal • EA: 5.2° vertical / 10.4° horizontal	Quantitative values of section 4
2 SD Ellipse	Ellipse of axes 2 SD in vertical and horizontal directions. • OS: 10.8° vertical / 17.6° horizontal • EA: 10.4° vertical / 20.8° horizontal	Quantitative values of section 4
Road Surface	Whole road surface of the lane ahead of vehicle to horizon	Uchida[8] JTC-1, CIE 2012 conference, Hangzhou
Window Area	Area of windscreen	JTC-1, CIE 2012 conference, Hangzhou

Table 4. Results of signal detection comparing the primitive shape centred at the horizon of the lane ahead to centred at the data for the residential road EA.

Shape	Centred at / on	Fpr	Tpr	f1-score
10° / 20° Ellipse	horizon of lane centre	0.04	0.79	0.60
	centre of recorded gaze locations	0.04	0.85	0.64
10° Circle	horizon of lane centre	0.02	0.52	0.55
	centre of recorded gaze locations	0.01	0.66	0.67

Table 5. Short summary of previous eye-tracking studies analysing the eye movement of drivers.

Study	**Method**	**Test participants**	
		Number	**Age (years) and reported experience**
Mourant and Rockwell, 1970[2]	Eye-tracking while driving in daylight	8	21-31 y experience not reported
Mourant and Rockwell, 1972[19]	Eye-tracking while driving in daylight	10	6 novice (16-17 y), 4 experienced (21-43 y)
Land and Lee, 1994[4]	Eye-tracking while driving in daylight	3	all experienced (no age given)
Maltz and Shinar, 1999[17]	Eye-tracking while observing four photographs of road scenes	10	5 younger (20-30 y) 5 older (62-80 y) experience not reported
Falkmer and Gregersen, 2005[20]	Eye-tracking while driving in daylight	40	20 learners (mean = 20 y), 20 experienced (mean = 35 y)
Cengiz et al., 2013[7]	Eye-tracking while driving in daylight and after dark	3	22 - 27 y; one experienced (driving > 100,000 km) and two less experienced (driving < 30,000 km)